Simulation of a Linear Permanent Magnet Vernier Machine for Direct-drive Wave Power Generation

Wenlong Li and K.T. Chau
Department of Electrical and Electronic Engineering,
The University of Hong Kong, Hong Kong
E-mail: wlli@eee.hku.hk

Abstract — This paper proposes a linear permanent magnet (PM) vernier machine for direct-drive wave power generation. Firstly, the machine structure is proposed and its parameters are indentified by finite element analysis (FEA). Secondly, the mathematical modeling of wave power absorption system was established. The control strategy for maximizing absorbed wave power is discussed. Then, by using Matlab/Simulink, the wave power generator system is modeled and simulated. A vector control scheme is implemented which controls power flow between the generator and the load via a bi-directional AC/DC converter. The simulation results verify the feasibility of the proposed machine used for direct-drive wave power generation.

I. INTRODUCTION

With increasing concerns on crude oil exhaustion and environment deterioration, clean and renewable energy exploitation and its related industrials develop in an accelerated pace [1]-[9]. Renewable energy such as wind energy and wave energy features as a variable speed and intermittent power source. In order to harvest this kind of energy, various permanent magnet machines with special structure and distinct merits were developed, such as doubly salient permanent magnet (DSPM) machine [10]-[17], permanent magnet hybrid brushless (PMHB) machine [18]-[25], double-stator cup-rotor permanent magnet machine [26]-[29], doubly salient memory machine [30]-[33], transverse-flux permanent magnet (TFPM) machine [34], [35], magnetic-geared permanent magnet brushless machine [36]-[47], etc. The last two types are aim to apply in a low-speed and high-torque density direct-drive applications which is more popular in recent years.

However, the complicated structure and the low power factor are two major drawbacks of the TFPM machine which result in a high initial cost and a low power efficiency. By integrated with a magnetic gear, the conventional high speed and high efficiency machine can satisfy the direct-drive application [38], [42], [46] and retain its merits at the same time. Nevertheless, the magnetic-geared machine has two moving bodies and three air-gaps which is also not easy to fabricate. Based on the concept of field modulation in magnetic gears, a PM vernier machine has been proposed to solve this problem [48]. By using a toothed-pole structure, which is equivalent to the field modulation ring of the magnetic gear combined with the stator, this machine can adopt only one moving body and one air-gap to achieve the same performance as the magnetic geared machine, thus it will be very competitive for direct-drive application.

The purpose of this paper is to extend the concept of PM vernier machines to its linear morphology and examine its performance in direct-drive wave power generation. By using FEM, the parameters of the linear vernier machine are indentified. Then based on Matlab/Simulink, the wave power generation system operation is simulated. The output power of the system is maximized with an appropriate control strategy.

II. LINEAR VERNIER MACHINE

As shown in Fig. 1, the vernier structure usually involves a toothed-pole structure which can interact with a different pole-pair number magnetomotive force (MMF) on the rotor. When the armature winding is assumed to have a pole-pair number of P, the fundamental MMF waveform of the armature excitation is given by:

$$f_a = F_a \cos(P(\theta - \omega t) + \theta_{a0}) \tag{1}$$

where F_a is the amplitude of the fundamental MMF waveform, ω is the angular frequency of the current in the armature winding, and θ_{a0} is the initial phase angle.

By omitting its DC offset component, the fundamental permeance of stator toothed-pole structure is:

$$\lambda_t = \Lambda_t \cos(Z_1\theta + \theta_{t0}) \tag{2}$$

where Λ_t is the amplitude of the stator teeth permeance waveform, Z_1 the number of the stator teeth, and θ_{t0} is the initial phase angle.

Thus, flux density in the air-gap due to interaction between armature excitation and the toothed pole stator can be simply decided by the following equation:

$$\begin{aligned} B_{ag} &= f_a \times \lambda_t \\ &= \Lambda_t F_a \{\cos[(Z_1 + P)\theta + \theta_{t0} - P\omega t + \theta_{a0}]\} \times \\ &\{\cos[(Z_1 - P)\theta + \theta_{t0} + P\omega t - \theta_{a0}]\} \end{aligned} \tag{3}$$

According to (3), it can be observed that the pole-pair number of field in air-gap has been changed by vernier structure. Thus, a steady force can be developed, if the PM pole-number Z_2 on the rotor satisfies the following relationship:

$$Z_2 = |Z_1 \pm P| \tag{4}$$

When ac current with an angular frequency ω runs in the armature windings, the resultant magnetic field of armature excitation rotates at a speed of ω/P, and the rotor speed is ω/Z_2. By borrowing concept of gear ratio in magnetic gear, the

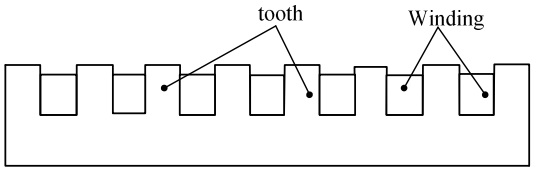

(a) Open-slot configuration

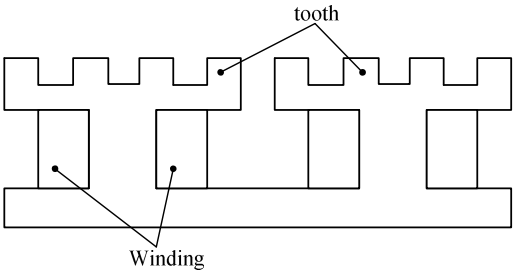

(b) Pole-split configuration

Fig. 1. Two types stator configuration for vernier structure.

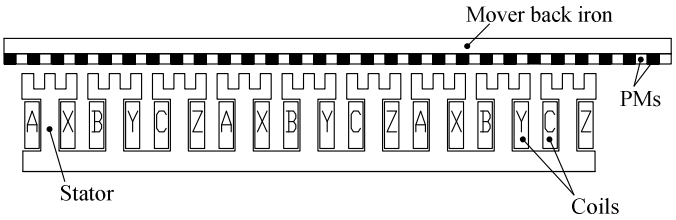

Fig. 2. Proposed linear permanent magnet machine for direct-drive wave power generation.

TABLE I
LINEAR PERMANENT MAGNET VERNIER MACHINE PARAMETERS

Items	Value
Rated voltage (RMS)	60 V
Rated current (RMS)	5.6 A
Rated power	1 kVA
Phase number	3
PM remanence	1.2 T
PM coercivity	940 kA/m
Air-gap length	1 mm
Pole pitch	6.5 mm
Phase resistance	2.8 Ω
Direct-axis inductance	54.2 mH
Quadrature inductance	54.2 mH
Translator mass	3.2 kg

gear ratio of this machine is Z_2/P. A small movement of the mover can cause a distinguished variation in flux linkage which can develop a high torque.

Two kinds of stator structure configuration is shown in Fig. 1, namely open-slot type and pole-split type [49]. The proposed machine adopts the latter one for a compact design as depicted in Fig. 2. It has a flat single-sided structure, which consists of 9 stator teeth splitting into 27 small teeth at the end, 24 active PM pole-pairs on the mover and 9 slots for housing 3-phase windings. The longitudinal-magnetized PMs are surface mounted on the mover back iron. The windings

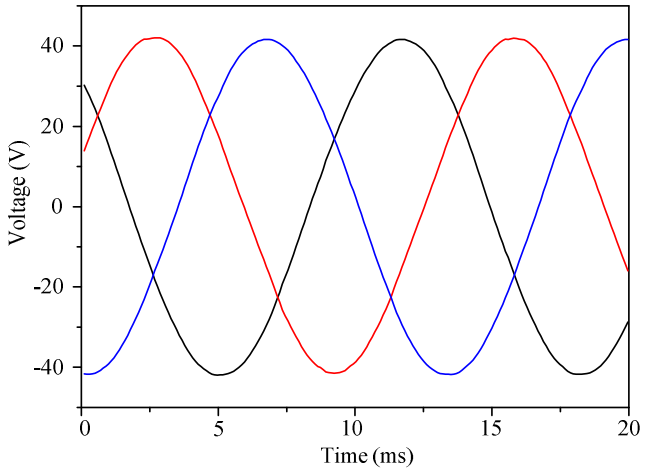

Fig. 3. Induced voltage waveforms of the proposed machine.

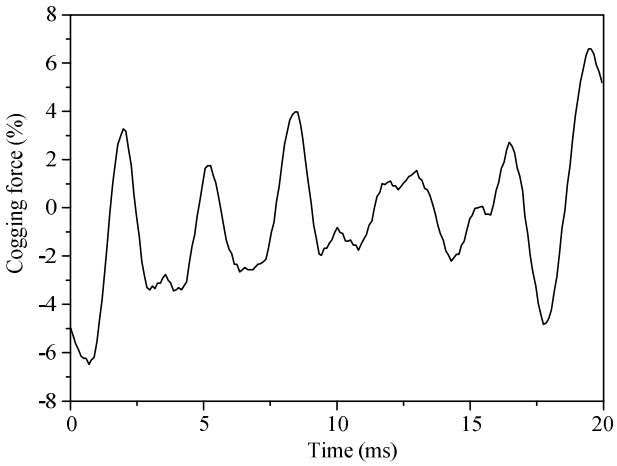

Fig. 4. Cogging force waveform of the proposed machine.

adopt a concentrated winding which can minimize end windings and ease the fabrication. The stator is artfully design that each inner stator tooth splits 3 small teeth which has the same function as flux modulation poles in magnetic gears.

In order to access the proposed machine performance, the finite element method (FEM) is applied for magnetic field calculation. Fig. 3 shows the no-load electromotive force (EMF) when the translator moves at a constant speed of 0.5 m/s. Fig.4 shows the cogging force of the proposed machine. It can be found that the cogging force is within 8% of the rated developed force which is very promising in direct-drive applications. The proposed machine parameters are listed in Table I.

III. MATHEMATICAL MODELING OF WAVE POWER ABSORPTION

The Ocean is a great treasure trove on earth. The wave energy resource in the ocean is considered as a tremendous alternative energy source for people in the coming years. In those wave energy conversion techniques, the direct-drive wave energy converter which engages a linear electrical generator for electric power production attracts more and more attention. Since this technique can directly couple linear electrical generator to the marine device such as buoy, float, or

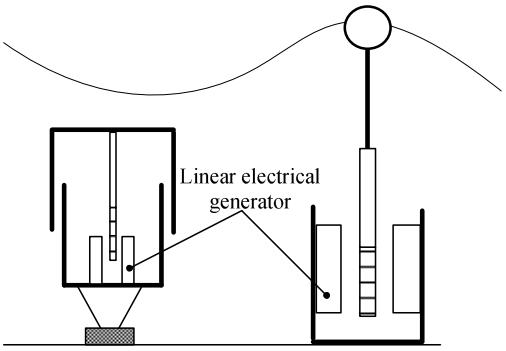

(a) Archimedes wave swing (b) Buoy-based type

Fig. 5. Two type direct-drive wave energy converters. (a) Archimedes wave swing. (b) Buoy-based type.

air-chamber for absorbing wave power along with the wave rise and fall, the energy efficiency is relatively higher than those indirect-drive approaches. Fig.3 shows two famous direct-drive wave energy converters which use the linear electrical generator for electricity generation. The first one is the Archimedes wave swing (AWS) which operates totally under the water [50]. The latter one is buoy-based wave energy converter. In this paper, the system adopts the buoy based one which is also called point absorber. Fig.4 shows the whole buoy-based direct-drive wave power generator system. The generator translator motion equation is given by [51]:

$$F_e + F_r + F_f + F_{em} = m\frac{d^2x}{dt^2} \tag{5}$$

where F_e is the incident wave force on the buoy, F_r is the radiated force of buoy acting on the water, F_f is the force due to friction between mechanical parts and the water, F_{em} is the electromagnetic force of the linear generator, m is the mass of the total moving part, and x is the displacement of the moving part.

By multiplying the velocity to (5), the power equation of the system can be described as below:

$$P_e - P_r - P_f - P_{em} = m\frac{dx}{dt}\frac{d^2x}{dt^2} \tag{6}$$

The power P_e, P_r, P_f, and P_{em} are developed by force F_e, F_r, F_f and F_{em}, respectively. The power P_r is the radiated power that returns to the sea from the buoy which is similar as the reactive power in electrical circuits. The power F_f is consumed by friction and P_{em} is the power absorbed by the generator and its load which is the key part of wave energy conversion.

In order to obtain the maximal absorbed power P_{em}, the radiated power P_r and the power P_f due to friction should be minimized when the incident wave power P_e keeps as a constant. The absorbed wave power by the proposed linear machine can be expressed as:

$$\tilde{P}_{em} = \tilde{F}_{em} \cdot \tilde{v}_t \tag{7}$$

where v_t is the velocity of the linear generator translator, and "~" denotes the variable is a complex variable.

According to (7), the generator force F_{em} should be controlled in phase with the speed of the translator v_t, thus the absorbed power P_{em} can be maximized [52]. It means that the current should be injected from the load part to satisfy the above condition.

IV. Simulation for Wave Power Generation with Matlab/Simulink

As discussed in section III, the generator force F_{em} should be controlled with the translator speed v_t for maximizing the wave power absorption. In order to regulate the generator force of the generator, a bi-directional AC/DC converter is deployed between the generator and the load.

The voltage, flux linkage and force equations of the linear generator in *d-q* reference frame are given as below:

$$u_d + R_a \cdot i_d + \frac{d\lambda_d}{dt} - \omega_t \cdot \lambda_q = 0 \tag{8}$$

$$u_q + R_a \cdot i_q + \frac{d\lambda_q}{dt} + \omega_t \cdot \lambda_d = 0 \tag{9}$$

$$\lambda_d = L_d \cdot i_d - \lambda_{pm} \tag{10}$$

$$\lambda_q = L_q \cdot i_q \tag{11}$$

$$F_{em} = \frac{3\pi}{2\tau_{pm}}[i_d \cdot i_q \cdot (L_d - L_q) - \lambda_{pm} \cdot i_q] \tag{12}$$

where u_d, u_q, i_d, i_q, λ_d and λ_q are the terminal voltage, current, flux linkage of the direct-axis and quadrature-axis, respectively, R_a is the armature winding resistance, ω_t is the translator velocity in radian per second, λ_{pm} is the flux linkage due to permanent magnet, τ_{pm} is the pole-pitch of permanent magnets on the translator.

The mathematical model of the linear generator is built by Matlab/Simulink according to (8)-(12) with the parameters listed in Table I. In order to control the generator force, the space vector control strategy is adopted which need to maintain the direct-axis current as zero. Thus, according to (12), the generator force is only a function of the quadrature-axis current [53]. The quadrature-axis current reference signal can be decided based on (7) and (12) as following:

$$i_q^* = \frac{c\tilde{v}_t}{\lambda_{pm}}\frac{2\tau_{pm}}{3\pi} \tag{13}$$

where c is a constant depend on the system.

Fig. 6 illustrates the whole system control block diagram. The proposed linear vernier machine is connected to a rechargeable battery system via a bi-directional AC/DC converter. The control system uses only current loop control to achieve the maximal power absorption. From encoder signal, the translator velocity v_t and its position can be estimated. With the translator velocity information, the reference signal of quadrature-axis current i_q^* can be calculated. With the position information, an abc/dq0 transformation for the direct-axis and quadrature-axis current reference signal can be achieved. By comparing the actual current signal with the current reference signal, the error signals are put to a hysteresis current regulator for generating a set of control pulse signal. With these firing signals, the power switches are turned on and off at the right time for tracing the reference signal.

Fig. 7 shows the translator velocity waveform when a sinusoidal external force acts on the system. Fig. 8 depicts the 3-phase no-load voltage waveforms. When the proposed linear generator is connected to the rechargeable battery system via the bi-directional AC/DC converter, the power extraction of the proposed generator can be maximized by aforementioned

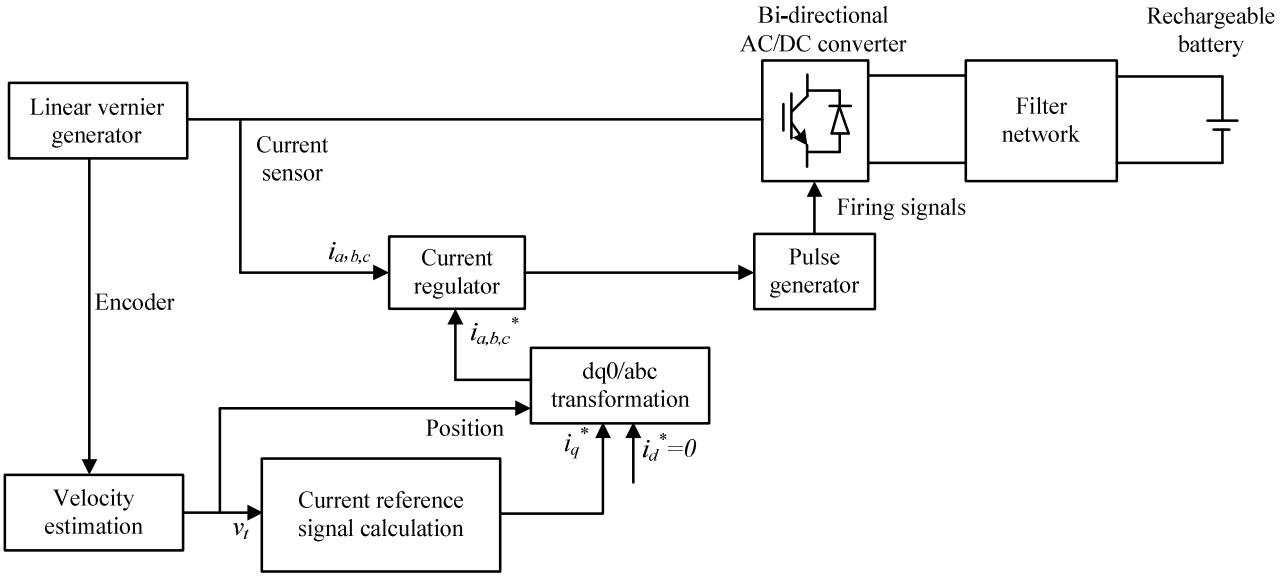

Fig. 6. System control diagram.

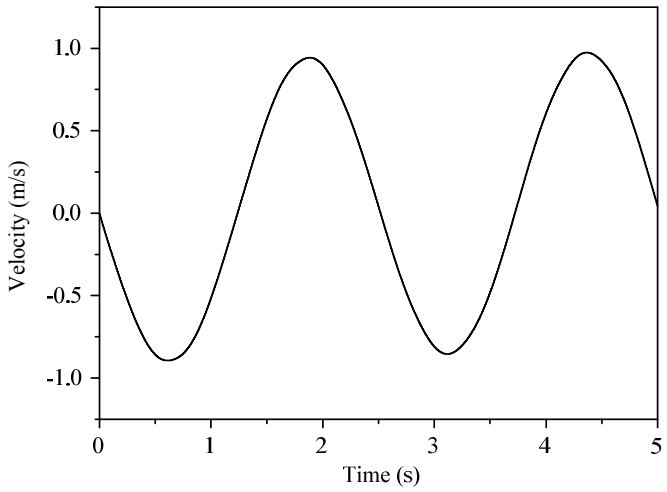

Fig. 7. The translator speed wavform.

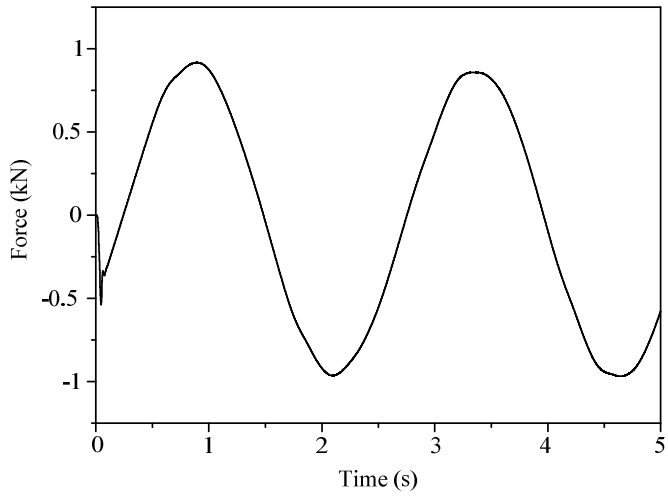

Fig. 9. The generator force waveform.

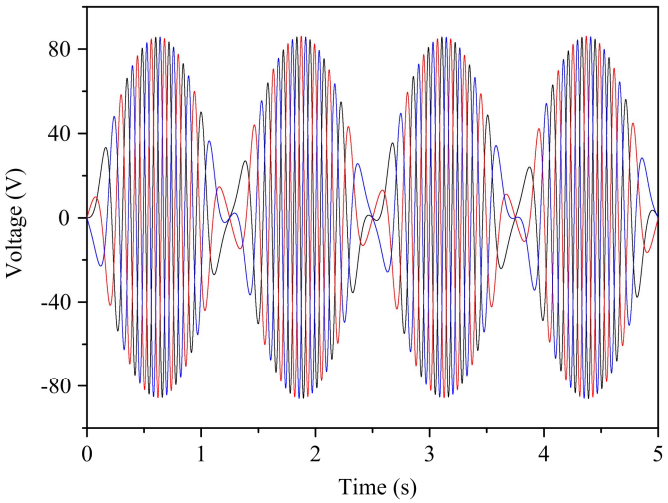

Fig. 8. 3-phase no-load voltage waveforms.

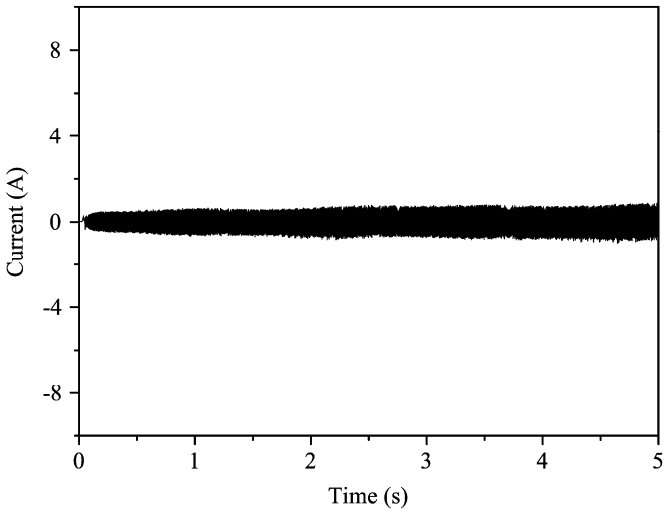

Fig. 10. The direct-axis current waveform.

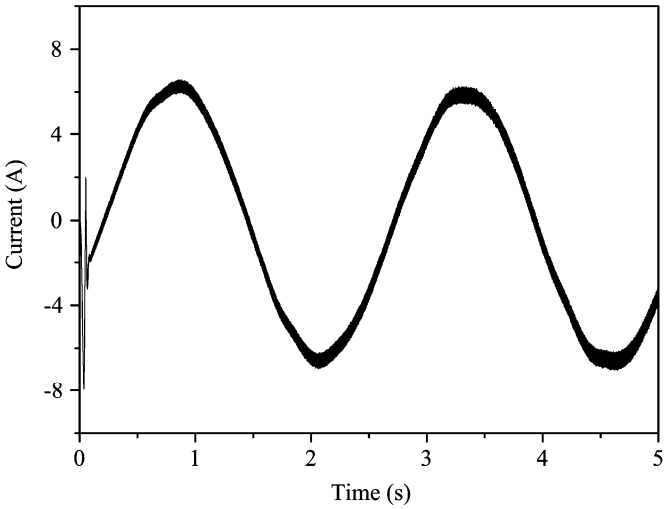

Fig. 11. The quadrature-axis current waveform.

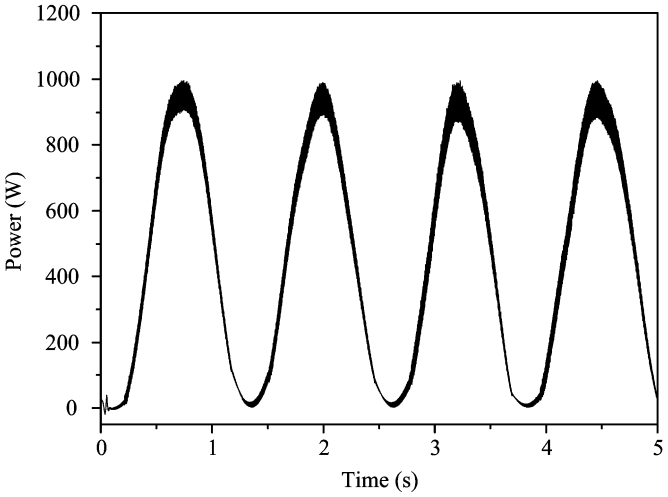

Fig. 12. The power generated by the proposed machine.

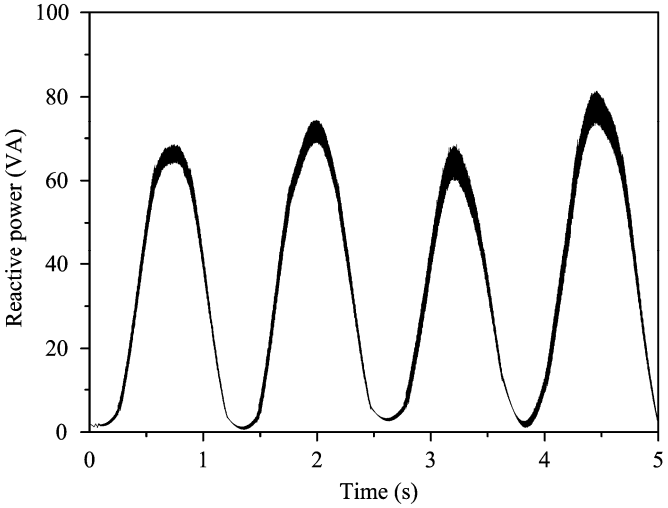

Fig. 13. The reactive power generated by the proposed machine.

vector control strategy. The generator force F_{em} waveform is shown in Fig. 9. It can be observed that the generator force F_{em} is almost controlled in phase with the translator speed, thus the maximal wave power absorption can be resulted. Fig. 10 and Fig. 11 show the controlled direct-axis and quadrature-axis current waveforms which both trace the reference signals very well. Fig. 12 and Fig. 13 depict the active power and reactive power generated by the propose generator. It can be found that the generated power can achieve a peak value of l kW with the maximal power absorption control strategy.

V. Conclusion

This paper proposes a low-speed and high force density linear permanent magnet vernier machine for the direct-drive wave power generation. By using FEM, the machine performance and its parameters are calculated. For maximizing the absorbed wave power, conditions for the generator operation are discussed. At last, the proposed machine and the control strategy are simulated by Matlab/ Simulink. The simulation results verify the feasibility of the proposed machine and its control strategy for maximal wave power absorption.

Acknowledgment

This work was supported by a grant (Project No. HKU710710E) from the Hong Kong Research Grants Council, Hong Kong Special Administrative Region, China.

References

[1] C.C. Chan and K.T. Chau, *Modern Electric Vehicle Technology*. Oxford University Press, November 2001, 352 pages.

[2] C.C. Chan, J.Z. Jiang, G.H. Chen, X.Y. Wang and K.T. Chau, "A novel polyphase multipole square-wave permanent magnet motor drive for electric vehicles," *IEEE Transactions on Industry Applications*, vol. 30, no. 5, September 1994, pp. 1258-1266.

[3] C.C. Chan, K.T. Chau, J.Z. Jiang, W. Xia, M. Zhu and R. Zhang, "Novel permanent magnet motor drives for electric vehicles," *IEEE Transactions on Industrial Electronics*, vol. 43, no. 2, April 1996, pp. 331-339.

[4] K.T. Chau, C.C. Chau, and C. Liu, "Overview of permanent magnet brushless drives for electric and hybrid electric vehicles," *IEEE Transactions on Industrial Electronics*, vol. 55, no. 6, pp. 2246-2257, June 2008.

[5] X. Zhang and K.T. Chau, "An automotive thermoelectric-photovoltaic hybrid energy system using maximum power point tracking," *Energy Conversion and Management*, vol. 52, no. 1, January 2011, pp. 641-647.

[6] X. Zhang and K.T. Chau, "Design and implementation of a new thermoelectric-photovoltaic hybrid energy system for hybrid electric vehicles," *Electric Power Components and Systems*, vol. 39, no. 6, April 2011, pp. 511-525.

[7] J. Gan, K.T. Chau, C.C. Chan and J.Z. Jiang, "A new surface-inset, permanent-magnet, brushless DC motor drive for electric vehicles," *IEEE Transactions on Magnetics*, vol. 36, no. 5, September 2000, pp. 3810-3818.

[8] S.Z. Jiang, K.T. Chau and C.C. Chan, "Spectral analysis of a new six-phase pole-changing induction motor drive for electric vehicles," *IEEE Transactions on Industrial Electronics*, vol. 50, no. 1, February 2003, pp. 123-131.

[9] K.T. Chau, W. Cui, J.Z. Jiang and Z. Wang, "Design of permanent magnet brushless motors with asymmetric air gap for electric vehicles," *Journal of Applied Physics*, vol. 99, no. 8, April 2006, paper no. 80R322, pp. 1-3.

[10] Y. Liao, F. Liang, and T.A. Lipo, "A novel permanent magnet motor with doubly salient structure," *IEEE Transactions on Idustry Applications*, vol. 31, no.5, September/October 1995, pp.1069-1078.

[11] K.T. Chau, M. Cheng, and C.C. Chan, "Performance analysis of 8/6-pole doubly salient permanent magnet motor," *Electric Machines and Power Systems*, vol. 27, no. 10, October 1999, pp. 1055-1067.

[12] M. Cheng, K.T. Chau, and C.C. Chan, "Design and analysis of a new doubly salient permanent magnet motor," *IEEE Transactions on Magnetics*, vol. 37, no. 4, July 2001, pp. 3012-3020.

[13] K.T. Chau, J.Z Jiang and Y. Wang, "A novel stator doubly fed doubly salient permanent magnet brushless machine," *IEEE Transactions on Magnetics*, vol. 39, no. 5, September 2003, pp. 3001-3003.

[14] K.T. Chau, Q. Sun, Y. Fan and M. Cheng, "Torque ripple minimization of doubly salient permanent magnet motors," *IEEE Transactions on Energy Conversion*, vol. 20, no. 2, June 2005, pp. 352-358.

[15] Y. Fan, K.T. Chau and M. Cheng, "A new three-phase doubly salient permanent magnet machine for wind power generation," *IEEE Transactions on Industry Applications*, vol. 42, no. 1, January/February 2006, pp. 53-60.

[16] Y. Fan, K.T. Chau and S. Niu, "Development of a new brushless doubly fed doubly salient machine for wind power generation," *IEEE Transactions on Magnetics*, vol. 42, no. 10, October 2006, pp. 3455-3457.

[17] K.T. Chau, Y.B. Li, J.Z. Jiang and C. Liu, "Design and analysis of a stator-doubly-fed doubly-salient permanent-magnet machine for automotive engines," *IEEE Transactions on Magnetics*, vol. 42, no. 10, October 2006, pp. 3470-3472.

[18] X. Luo, and T.A. Lipo, "A synchronous/permanent magnet hybrid AC machine," *IEEE Transactions on Energy Conversion*, vol. 15, no. 2, June 2000, pp. 203-210.

[19] K.T. Chau, Y.B. Li, J.Z. Jiang and S. Niu, "Design and control of a PM brushless hybrid generator for wind power application," *IEEE Transactions on Magnetics*, vol. 42, no. 10, October 2006, pp. 3497-3499.

[20] C. Liu, K.T. Chau, J.Z. Jiang and S. Niu, "Comparison of stator-permanent-magnet brushless machines," *IEEE Transactions on Magnetics*, vol. 44, no. 11, November 2008, pp. 4405-4408.

[21] C. Liu, K.T. Chau, W. Li and C. Yu, "Efficiency optimization of a permanent-magnet hybrid brushless machine using dc field current control," *IEEE Transactions on Magnetics*, vol. 45, no. 10, October 2009, pp. 4652-4655.

[22] C. Liu, K.T. Chau and X. Zhang, "An efficient wind-photovoltaic hybrid generation system using doubly-excited permanent-magnet brushless machine," *IEEE Transactions on Industrial Electronics*, vol. 57, no. 3, March 2010, pp. 831-839.

[23] C. Liu and K.T. Chau, "Loss analysis of permanent magnet hybrid brushless machines with and without HTS field windings," *IEEE Transactions on Applied Superconductivity*, vol. 20, no. 3, June 2010, pp. 1077-1080.

[24] C. Liu, K.T. Chau and W. Li, "Comparison of fault-tolerant operations for permanent-magnet hybrid brushless motor drive," *IEEE Transactions on Magnetics*, vol. 45, no. 6, June 2010, pp. 1378-1381.

[25] C. Liu, K.T. Chau, and J.Z. Jiang, "A permanent-magnet hybrid brushless integrated- starter-generator for hybrid electric vehicles," *IEEE Transactions on Industrial Electronics*, vol. 57, no. 12, pp. 4055-4064, December 2010.

[26] S. Niu, K.T. Chau, J.Z. Jiang and C. Liu, "Design and control of a new double-stator cup-rotor permanent-magnet machine for wind power generation," *IEEE Transactions on Magnetics*, vol. 43, no. 6, June 2007, pp. 2501-2503.

[27] S. Niu, K.T. Chau and J.Z. Jiang, "Analysis of eddy-current loss in a double-stator cup-rotor PM machine," *IEEE Transactions on Magnetics*, vol. 44, no. 11, November 2008, pp. 4401-4404.

[28] S. Niu, K.T. Chau and C. Yu, "Quantitative comparison of double-stator and traditional permanent magnet brushless machines," *Journal of Applied Physics*, vol. 105, no. 7, April 2009, paper no. 07F105, pp. 1-3.

[29] S. Niu, K.T. Chau, J. Li and W. Li, "Eddy current analysis of double-stator inset-type permanent magnet brushless machines," *IEEE Transactions on Applied Superconductivity*, vol. 20, no. 3, June 2010, pp. 1097-1101.

[30] C. Yu, K.T. Chau, X. Liu and J.Z. Jiang, "A flux-mnemonic permanent magnet brushless motor for electric vehicles," *Journal of Applied Physics*, vol. 103, no. 7, April 2008, paper no. 07F103, pp. 1-3.

[31] C. Yu, K.T. Chau and J. Z. Jiang, "A flux-mnemonic permanent magnet brushless machine for wind power generation," *Journal of Applied Physics*, vol. 105, no. 7, April 2009, paper no. 07F114, pp. 1-3.

[32] Y. Gong, K.T. Chau, J.Z. Jiang, C. Yu and W. Li, "Analysis of doubly salient memory motors using Preisach theory," *IEEE Transactions on Magnetics*, vol. 45, no. 10, October 2009, pp. 4676-4679.

[33] C. Yu and K.T.Chau, "Design, analysis and control of DC-excited memory motors," *IEEE Transactions on Energy Conversion*, vol. 26, no. 2, June 2011, pp. 479-489.

[34] J. Wang, K.T. Chau, J.Z. Jiang and C. Yu, "Design and analysis of a transverse flux permanent magnet machine using three dimensional scalar magnetic potential finite element method," *Journal of Applied Physics*, vol. 103, no. 7, April 2008, paper no. 7F107, pp. 1-3.

[35] W. Li and K.T. Chau, "Design and analysis of a novel linear transverse flux permanent magnet motor using HTS magnetic shielding," *IEEE Transactions on Applied Superconductivity*, vol. 20, no. 3, June 2010, pp. 1106-1109.

[36] K. Atallah and D. Howe, "A novel high-performance magnetic gear," *IEEE Transactions on Magnetics*, vol. 37, no. 4, July 2001, pp. 2844-2846.

[37] K. Atallah, S.D. Calverley, and D. Howe, "Design, analysis and realization of a high-performance magnetic gear", *IEE Proceedings of Electric Power Applications*, vol. 151, no. 2, March 2004, pp. 135-143.

[38] K.T. Chau, D. Zhang, J.Z. Jiang, C. Liu and Y.J. Zhang, "Design of a magnetic-geared outer-rotor permanent-magnet brushless motor for electric vehicles," *IEEE Transactions on Magnetics*, vol. 43, no. 6, June 2007, pp. 2504-2506.

[39] K.T. Chau, D. Zhang, J.Z. Jiang and L. Jian, "Transient analysis of coaxial magnetic gears using finite element comodeling," *Journal of Applied Physics*, vol. 103, no. 7, April 2008, paper no. 07F101, pp. 1-3.

[40] X. Liu, K.T. Chau, J.Z. Jiang and C. Yu, "Design and analysis of interior-magnet outer-rotor concentric magnetic gears," *Journal of Applied Physics*, vol. 105, no. 7, April 2009, paper no. 07F101, pp. 1-3.

[41] L. Jian and K.T. Chau, "Analytical calculation of magnetic field distribution in coaxial magnetic gears," *Progress In Electromagnetics Research*, vol. 92, 2009, pp. 1-16.

[42] L. Jian, K.T. Chau and J.Z. Jiang, "A magnetic-geared outer-rotor permanent-magnet brushless machine for wind power generation," *IEEE Transactions on Industry Applications*, vol. 45, no. 3, May/June 2009, pp. 954-962.

[43] L. Jian, K.T. Chau, Y. Gong, J.Z. Jiang, C. Yu and W. Li, "Comparison of coaxial magnetic gears with different topologies," *IEEE Transactions on Magnetics*, vol. 45, no. 10, October 2009, pp. 4526-4529.

[44] L. Jian, K.T. Chau, W. Li and J. Li, "A novel coaxial magnetic gear using bulk HTS for industrial applications," *IEEE Transactions on Applied Superconductivity*, vol. 20, no. 3, June 2010, pp. 981-984.

[45] L. Jian and K.T. Chau, "Design and analysis of a magnetic-geared electronic-continuously variable transmission system using finite element method," *Progress In Electromagnetics Research*, vol. 107, 2010, pp. 47-61.

[46] W. Li and K.T. Chau, "A linear magnetic-geared free-piston generator for range-extended electric vehicles," *Journal of Asian Electric Vehicles*, vol. 8, no. 1, June 2010, pp. 1345-1350.

[47] W. Li, K.T. Chau and J. Li, "Simulation of a tubular linear magnetic gear using HTS bulks for field modulation," *IEEE Transactions on Applied Superconductivity*, vol. 21, no. 3, June 2011, pp. 1167-1170.

[48] J. Li, K.T. Chau, J.Z. Jiang, C. Liu and W. Li, "A new efficient permanent-magnet vernier machine for wind power generation," *IEEE Transactions on Magnetics*, vol. 45, no. 6, June 2010, pp. 1475-1478.

[49] A. Toba and T.A. Lipo, "Novel dual-excitation permanent magnet vernier machine," *Proceeding of IEEE Industry Applications Conference*, vol. 4, 1999, pp: 2539-2544.

[50] D. Valerio, P. Beirao, and J.S. Costa, "Optimisation of wave energy extraction with the Archimedes Wave Swing," vol. 34, no. 17-18, December 2007, pp. 2330-2344.

[51] J. Falnes, *Ocean waves and oscillating systems: Linear interactions including wave-energy extraction*. Cambridge University Press. 2002, 275 pages.

[52] J. Vining, T.A. Lipo, and G. Venkataramanan, "Self-synchronous control of doubly-fed linear generators for ocean wave energy applications," *IEEE Energy Conversion Congress and Exposition*, 2010, pp. 2386-2391.

[53] V.D. Colli, P. Cancelliere, F. Marignetti, R.D. Stefano, and M. Scarano, "A tubular-generator drive for wave energy conversion," *IEEE Transactions on Industrial Electronics*, vol. 53, no. 4, August 2006, pp. 1152-1159.